



## Structural and Optical Study of Au Nanoparticles Incorporated in Al<sub>2</sub>O<sub>3</sub> and SiO<sub>2</sub> Thin Films Grown by RF-Sputtering

A. Belahmar, A. Chouiyakh

Department of Physics, Renewable Energy and Environment Laboratory, Faculty of Sciences Ibn Tofail University,  
P.O. Box 133, 1400, Kenitra, Morocco

**Abstract**— Gold nanoparticles (AuNPs) dispersed in SiO<sub>2</sub> and Al<sub>2</sub>O<sub>3</sub> films were deposited on glass substrate in the same conditions by RF-sputtering technique. The structural and optical properties were investigated with respect to the Au content in the two dielectric matrices. The phase composition of all the samples determined by X-ray diffraction revealed the existence of the Au nanoparticles in amorphous films, where the mean particles size of AuNPs varies depending on the host matrix and gold content. The optical absorption spectra of the Au/Al<sub>2</sub>O<sub>3</sub> samples showed a significant absorption bands due to surface plasmon resonance characteristic of gold nanoparticles in the range 500 – 530 nm, while no absorption peak was observed in the Au/SiO<sub>2</sub> nanocomposite films deposited at the same conditions. In addition, the incorporation of AuNPs in the silica and alumina films modifies considerably their transmission in the visible region, particularly in the alumina films. A red shift surface plasmon resonance band absorption characteristic of increase of Au particles in the case of alumina films is observed.

**Keywords**— Gold nanoparticles, Surface Plasmon Resonance, transmittance, sputtering

### I. INTRODUCTION

Gold nanoparticles (AuNPs), i.e. particles with the dimensions in the range of units to hundreds of nanometers, recently attract an extensive attention in various fields of chemistry, physics, material science, medicine, and photonics, due to their unique physical and chemical properties who are different from those of the corresponding bulk material (e. g [1]-[6]). In particular, when light impinges onto a metallic NP, its free conduction electrons may respond collectively by oscillating in resonance. This collective resonant excitation, which occurs in the visible range of the electromagnetic spectrum in the case of noble metals, is known a surface plasmon resonance (SPR). The corresponding peak absorption depends on the kind of the metal, the size, the shape, and the chemical environment of NPs. Modifying one of these parameters represents a way to control the optical properties of the corresponding composite materials (i.e., a matrix containing metallic NPs) (e.g. [7]- [11]). The problem of the absorption and scattering of light by spherical particles of arbitrary size was first treated by Mie, in 1908 (e.g. [12]). The author described theoretically the mechanism for the absorption of light by small metal particles solving the Maxwell's equations. The theory is based on an assumption that the interactions of the electromagnetic field with the particle induce a charge separation on its surface. This charge separation is a cause for an occurring restoring force. It has been shown that such absorption of light in the UV-Visible region by the metal particles is sensitive to many geometrical, as well as environmental factors (e.g. [13]). Based on the assumptions that the particles are spherical, small and embedded in an isotropic and non-absorbing medium, Mie calculated the absorption coefficient and found that its real part is:

$$\alpha(\lambda) = \frac{18\pi n_m^3}{\lambda} \frac{\varepsilon_2(\lambda)}{(\varepsilon_1(\lambda) + 2n_m^2)^2 + \varepsilon_2^2(\lambda)} \quad (1)$$

Where  $n_m$  is the refractive index of the matrix.  $\varepsilon_1(\lambda)$  and  $\varepsilon_2(\lambda)$  are the real and imaginary part of complex dielectric constant of Au nanoparticle ( $\varepsilon_{Au}$ ), respectively. The peak height is well approximated by  $\varepsilon_2(\lambda)$ . A resonance in the spectrum of  $\alpha(\lambda)$  will occur whenever:

$$\varepsilon_1(\lambda) = -2n_m^2 \quad (2)$$

According to Eq. (1), the plasmon absorption is size-independent within the dipole approximation. However, experimentally a size dependence of the surface plasmon absorption was early observed with decreasing of particle size. Contradicted with experimental observations, Mie's theory has evolved to include the fundamental assumption, that the dielectric function of the nanoparticle material is size dependent, when particle size becomes of the order of the mean free path of the conduction electrons, or even smaller (e.g. [14]-[16]). Size dependence for the quasi-static regime is introduced in Equation (1) by assuming a size-dependent material dielectric constant  $\varepsilon(\omega, r)$  (e.g. [17]):

$$\varepsilon_{Au}(\omega, r) = \varepsilon_{bulk}(\omega) + \frac{\omega_p^2}{\omega^2 + i\omega\Gamma_{bulk}} - \frac{\omega_p^2}{\omega^2 + i\omega(\Gamma_{bulk} + Av_F/r)} \quad (3)$$

Where  $\varepsilon_{bulk}(\omega)$ ,  $\omega_p$ ,  $v_F$ ,  $\Gamma_{bulk}$  and A, being the dielectric function, the plasmon frequency, the Fermi velocity, the damping constant of the bulk metal, and A is a phenomenological parameter including details of the scattering process, respectively. As the dielectric constant in the expression of absorption coefficient (denominator), hence the refractive index of the matrix plays a very important role in surface plasmon resonance (SPR). From the Eq. (1), one can deduce two limiting cases for which  $\alpha(\lambda)$  is equal to zero. In the first case, ( $\varepsilon_2(\lambda) \rightarrow \infty$ ), however, the material reflects all of

incoming radiation at this wavelength, that is the complex part of the dielectric function for metals has a large value in the visible making them very shiny and totally reflecting for the incoming light. In the second case, the complex part of the dielectric constant is zero ( $\epsilon_2(\lambda) = 0$ ), which is the particle is non-absorbing. This is the case of dielectric materials, as silica quartz ( $\text{SiO}_2$ ) or alumina sapphire ( $\text{Al}_2\text{O}_3$ ), which do not absorb in the visible-range.

The  $\text{Al}_2\text{O}_3$  is an insulating material, which is widely used in mechanical and optical applications, due to its excellent corrosion resistance, good mechanical strength and high hardness; as well as high transparency (e.g.[18]) and low refractive index around 1.7 (e.g.[19]). Actually,  $\text{Al}_2\text{O}_3$  is also an excellent material for sensing (e.g. [20]). On the other hand,  $\text{SiO}_2$  thin films are broadly used in various application fields such as passivation layers in electronic devices, protection, layers of magnetic or optical disks and anti-reflective coatings, because of their excellent chemical stability and optical transmittance with low refractive index (e.g. [21]–[22]).

Nanocomposite films consisting of metal particles such as gold embedded in a silica and alumina matrix have recently been the subject of many studies (e.g. [23]–[52]). Au/ $\text{SiO}_2$  and Au/ $\text{Al}_2\text{O}_3$  composite thin films have been fabricated using various methods, such ion implantation (e.g.[23]–[28]), sol-gel (e.g.[29]–[31]), Laser evaporation and cluster deposition (e.g.[32]–[35]), hybrid techniques combining pulsed-DC sputtering and PECVD, which is used for simultaneous Au sputtering and  $\text{SiO}_2$  deposition (e.g.[36]–[37]), and RF magnetron sputtering (e.g.[38]–[54]). Compared to ion-implantation processes, sputtering processes are much simpler and inexpensive. The flexibility that permits the fabrication of diverse metal–dielectric composite films with uniformly distributed metal particles is other advantages of the sputtering methods (e.g. [38]).

In this work, Au/ $\text{Al}_2\text{O}_3$  and Au/ $\text{SiO}_2$  nanocomposite films were synthesized on glass substrate at room temperature by RF-magnetron sputtering technique. The as-deposited films were characterized by X-ray diffraction and optical absorption spectroscopy.

## II. EXPERIMENTAL METHODS

RF-magnetron sputtering method was used to deposit thin films composed of Au clusters embedded in two different host matrices: aluminum oxide ( $\text{Al}_2\text{O}_3$ ) and silica oxide ( $\text{SiO}_2$ ). The composite thin films have been grown on glass substrates (ISO 8037) at room temperature in an argon gas at a constant working pressure of  $2.10^{-3}$  mbar, in an Alcatel SCM 650 sputtering system. In order to produce the Au/ $\text{Al}_2\text{O}_3$  films, a target consisted of pure (99.99%) metal Au chips (Goodfellow, UK) placed on top of a 50 mm diameter alumina disc (99.99%) covering a fraction of area is at 60 mm away from the substrates. In order to obtain the Au/ $\text{SiO}_2$  composite films, a similar procedure was used. Sputter deposition, in a radio frequency (13.56 MHz) machine, has been carried out after the chamber reached a base pressure of  $1.10^{-6}$  mbar. The relevant growth conditions of the films are shown in Table I.

Table I. Films Growth Conditions

Initial pressure (mbar)	$1.10^{-6}$
Working pressure (mbar)	$2.10^{-3}$
Au target (%)	1.3-2.6
Bias (V)	-50
Power (W)	50
Temperature	RT
Deposition time	4h30mn

Structural characterization of the composite films was performed in a Philips PW 1710 spectrometer using  $\text{Cu}_{K\alpha}$  radiation  $\lambda = 1.5406 \text{ \AA}$ . The diffraction patterns were collected over the range  $10^\circ$  to  $80^\circ$ . The identification of Au crystalline phases was done using the JCPDS database cards (no. 04-0784). Optical absorption spectra of composite films were registered by a Shimadzu UV 30101 PC spectrometer, in near ultra-violet-visible-near infra-red range (NUV-VIS-NIR) from 200 to 2000 nm.

## III. RESULTS AND DISCUSSION

### 3.1 Structural analysis

Fig. 1(a, b) shows the X-ray diffraction pattern of the samples deposited at 1.3% and 2.6% of materials from which the composite film is fabricated. X-ray diffractogram of gold thin film with a cubic structure, presented as a reference, is also reported in Fig.1. For  $r_{\text{Au}/\text{SiO}_2} = 1.3\%$ , the spectra of the sample don't reveal clearly diffraction peaks corresponding to Au or the silica material, but shows an intense broad band around  $2\theta = 26^\circ$  and a weak diffraction peak at  $2\theta = 38.5^\circ$ . When increasing the gold-to silica surface ratio to 2.6%, the XRD patterns exhibits a shoulder in the range  $35^\circ$ – $47^\circ$ , and a broad peak at  $2\theta = 64^\circ$ . It can be expected that the spectra of the composite films results from the superposition of two diffractograms, assigned to small gold particles and the amorphous silica matrix. It can be noted, that for  $r_{\text{Au}/\text{Al}_2\text{O}_3} = 1.3\%$ , the sample exhibits an XED spectra identical to that of Au/ $\text{SiO}_2$  deposited at  $r_{\text{Au}/\text{SiO}_2} = 2.6\%$ . However, as shown in Fig.1 (b), for  $r_{\text{Au}/\text{Al}_2\text{O}_3} = 2.6\%$ , the XRD pattern of the Au/ $\text{Al}_2\text{O}_3$  composite film reveals well- defined diffraction pattern whose much well with the diffraction peaks of bulk gold metal. We can note that the intensity of the Au diffraction peaks increases with increasing surface gold plate placed on top of the alumina or silica disc target, and the Au crystallites have an orientation along the Au (111) direction.

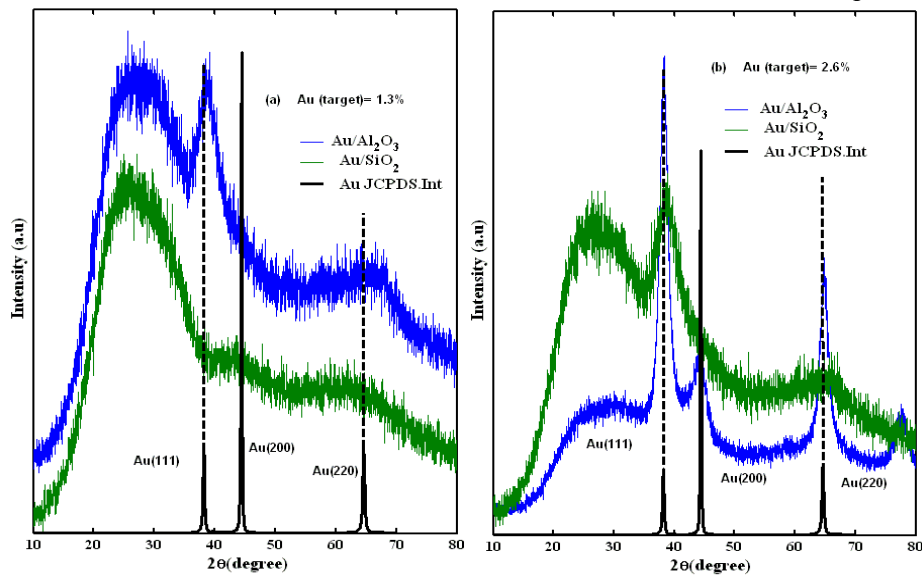


Fig. 1: Compare the XRD patterns of gold thin films Au/SiO<sub>2</sub> and Au/Al<sub>2</sub>O<sub>3</sub> composite deposited with different Au target (%)

To determine the phase structure, size, and lattice constant of AuNPs embedded in alumina and silica films, deconvolution procedure was used where details are reported elsewhere (e.g.[48]). The curve fitting of the XRD spectrum of the sample deposited at  $r_{Au/SiO_2} = 2.6\%$  is reported in Fig. 2. From the values of the Bragg angle position  $\theta_B$  and the full width at half maximum (FWHM) of the Au (111) reflection, we estimated the particle size (D) using the Debye-Scherrer's equation:

$$D = \frac{0.9\lambda}{(FWHM)\cos\theta_B} \quad (4)$$

Where  $\lambda$  is the wavelength of  $Cu_{K\alpha}$  radiation,  $\theta_B$  is the Bragg angle of the diffraction peak. The average size was found to be in the range 0.33 - 1.33nm for Au/SiO<sub>2</sub>, and 1.52 - 5.04 nm for Au/Al<sub>2</sub>O<sub>3</sub> when the gold-to dielectric surface ratio varies from 1.3% to 2.6%. Also, from XRD analysis, it was observed that lattice parameter is lower than that of the gold bulk and thereby the presence of compressive volume strain in the AuNPs. Table II summarizes the fitting parameters determined from the Au (111) orientation plane for all the samples.

Table II. Results of the Curves Fitting of the Experimental Diffractograms of the Samples Deposited At Various Au Target (%)

samples	Au (target)%	FWHM (degree)	2θ (degree)	Lattice parameter (Å)	size (nm)
$r_{Au/Al_2O_3}$	1.3	5.54	38.78	4.018	1.52
	2.6	1.67	38.29	4.068	5.04
$r_{Au/SiO_2}$	1.3	25.65	38.32	4.065	0.33
	2.6	7.42	38.68	4.028	1.13

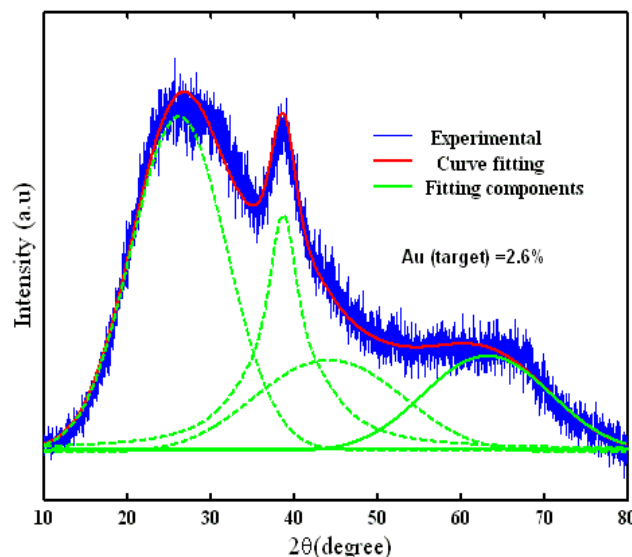


Fig. 2: Experimental diffractogram of Au /SiO<sub>2</sub> sample deposited at Au target (2.6%) and their curve fitting where different pseudo-Voigt functions were taken into account.

### 3.2 Optical studies

The corresponding optical properties of Au/SiO<sub>2</sub> and Au/Al<sub>2</sub>O<sub>3</sub> composite films were investigated by optical transmission spectroscopy. The transmittance spectra for all samples together with the glass substrate taking as a reference measured in wavelength range (200 –2000) nm are reported in Fig. 3. It was observed in the case of Au/SiO<sub>2</sub> composite films that the sample deposited at 1.3% and the glass substrate have the same transparency region. The absorption edge shifted to longer wavelengths up to 500 nm, as the gold to silica surface ratio increased to 2.6%. The transmittance of the Au/Al<sub>2</sub>O<sub>3</sub> films grown at 1.3% was about 65% in the region 500 – 800 nm, and 80% for the wavelengths higher than 1600nm, whereas the sample deposited at 2.6% remains opaque in the visible and the transparency drops to 40% at 1600 nm. Thus, the transmission spectra can be a sensitive measure of gold content in the films.

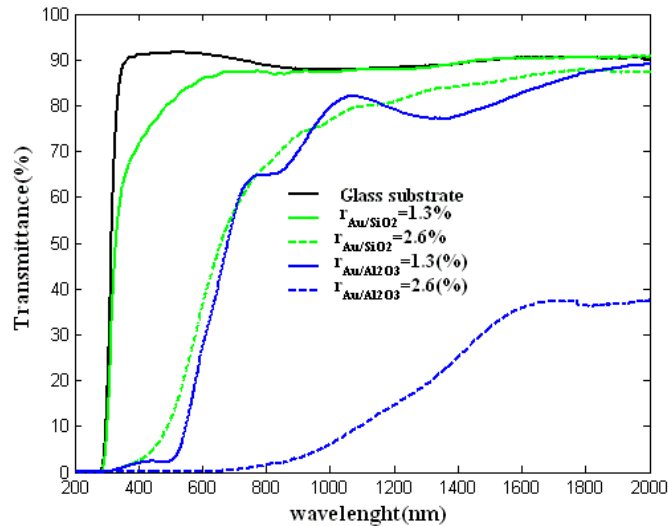


Fig. 3: Transmittance profiles of Au/SiO<sub>2</sub> (—) and Au/Al<sub>2</sub>O<sub>3</sub> (---) films for different Au target (%).

In order to further investigate the optical properties, it is necessary to study the optical absorption edge. The experimental absorption coefficient  $\alpha$  can be calculated from the following relation:

$$T = A \exp(-\alpha d) \quad (5)$$

Where T is the transmittance of thin film, A is a constant, and d is the film thickness. The constant A is approximately unity, as the reflectivity is negligible and insignificant near the absorption edge. Relation between direct band gap and the experimental absorption coefficient can be given by the following expression (e.g. [55])

$$\alpha h\nu = C(h\nu - E_g)^{1/2} \quad (6)$$

Where  $h$ , is the Planck constant,  $C$  is a constant for the direct transition,  $\nu$  is frequency of radiation and  $\alpha$  is the optical absorption coefficient. The optical absorption band gap  $E_g$  can be obtained from the intercept of  $(\alpha h\nu)^2$  versus photon energy ( $h\nu$ ). The optical gap deduced for the two kind of the films, decreases from 4eV to 3.7eV, when the Au target (%) increases. This result may be due to the fact that the formation of larger Au particles decreases the band gap energy of the composite films. The gap values found in this work are similar to those reported by the authors (e.g. [50]).

An important characteristic of the gold and other noble metal nanoparticles is the surface plasmon resonance, revealed by an absorption band, in the visible spectrum, which corresponds to the formation of metal nanoparticles, depending on the size and environment. To study the effect of surface plasmon resonance, in the transparency region, we start with the theoretical calculation of the absorption coefficient by a combination of Eq. (1) and Eq. (2). We use for gold nanoparticles, the values of  $\omega_p = 1.39 \cdot 10^{16} \text{ Hz}$ ,  $v_F = 1.4 \cdot 10^6 \text{ m/s}$ ,  $\Gamma_{bulk} = 1.4 \cdot 10^6 \text{ s}^{-1}$  and a value for  $A = 2$  (e.g. [48]) is required to extract the correct fitting parameters. The dielectric constant values of the bulk were taken from (e.g. [56]). Using Eq. (2) and by substituting the real part of the metal electric permittivity from Eq. (3), the position of the SPR resonance can be expressed as follows:

$$\omega_s = \frac{\omega_p}{\sqrt{2n_m^2 + \epsilon'_d(\omega_s)}} \quad (7)$$

The term  $\epsilon'_d$  refers to the real part of the dielectric function contributed by the core electrons (specially the d electrons).

On the other hand, Eq. (7) qualitatively describes a dependence of the SPR resonance on the dielectric properties of the host matrix, which the metal nanoparticles are incorporated in. An increase of dielectric constant (refractive index) evokes a shift of absorption maximum towards longer wavelengths (e.g. [57]-[59]). Smithard and Hosoya et al. found that the surrounding medium could bring great influence to the position of SPR peaks of the noble particles embedded in various matrices (e.g. [60]-[61]), and induce a spill-out effect of the electrons in the particle surface. The absorption coefficients of the Au particles embedded in different matrix have been calculated and the results are reported in Fig. 4. It is clearly seen that the SPR resonance maxima are more red-shifted for nanocomposites having a matrix with higher dielectric constant. We present, in Table III, the results obtained by our simulation.

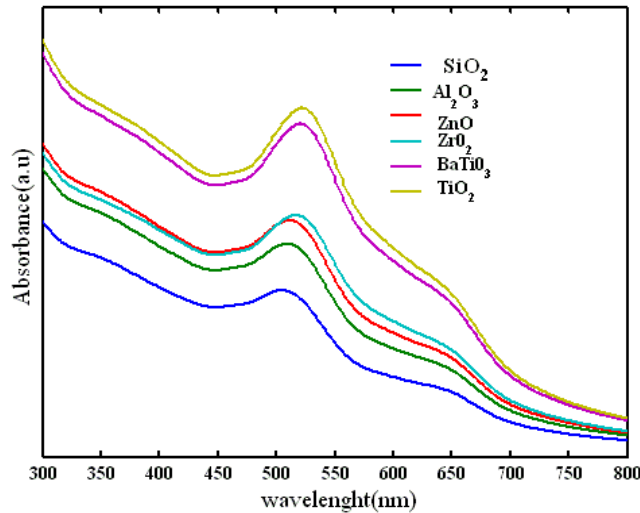


Fig.4: Spectral positions of SPRs of gold nanoparticles of 2.5 nm size embedded in various matrices.

Table III. The Numerical Results Corresponding To Fig.4

Matrix	Refractive index	SPR
SiO <sub>2</sub>	1.50	504
Al <sub>2</sub> O <sub>3</sub>	1.77	509
ZnO	1.90	511
ZrO <sub>2</sub>	2.20	517
BaTiO <sub>3</sub>	2.41	520
TiO <sub>2</sub>	2.49	522

The precise position, intensity and bandwidth of the SPR peak are not dependent only of the matrix, but also depend on size. Three discrete size domains, namely quantum (<2 nm), intrinsic (2–20 nm) and extrinsic (>20 nm) regimes and as such still forms the basis for significant scientific research (e.g. [1]). It is understood that for nanoparticles in the extrinsic regime, information concerning the precise nanostructure, specifically that of core size, can be inferred from the relative position of the SPR peak, with larger nanoparticles resulting in a red shift to lower energies(e.g.[14]). However, for particles smaller than 20 nm the situation becomes more complicated, with both red and blue shifts observed for nanoparticles in the intrinsic regime, most probably due to small particle effects, including discontinuous changes to band structure and ‘spill out’ of the conduction electrons ( e.g.[57]). Further confusion is added for particles in the quantum regime, where the SPR peak disappears due to the onset of quantum effects and strong damping of the plasmon oscillation as a result of low electron density in the conduction band (e.g. [62]).

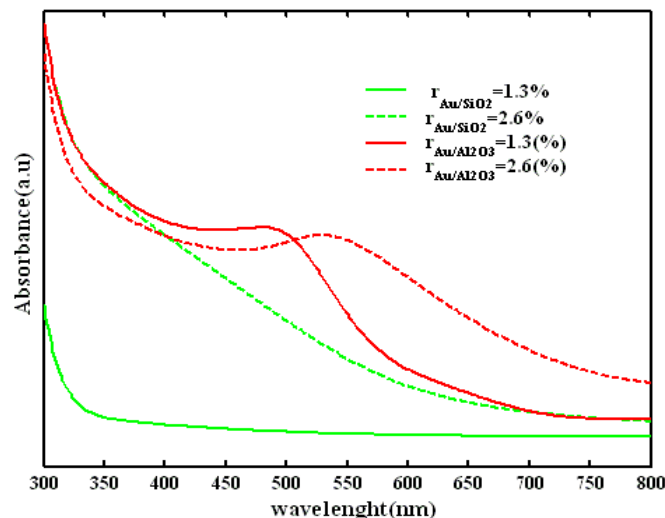


Fig. 5: Optical absorption of Au/SiO<sub>2</sub> (–) and Au/Al<sub>2</sub>O<sub>3</sub> (–) films for different Au target (%).

The absorption coefficients calculated from the transmittance of each sample has been plotted against wavelength are reported in Fig.5. In the figure, the Au/SiO<sub>2</sub> composite films show essentially decaying curves without the surface plasmon resonance peak. The nonappearance of an absorption peak in the sample can be associated to the AuNPs sizes smaller than 2 nm (e.g. [48]). In opposite, the Au/Al<sub>2</sub>O<sub>3</sub> films deposited at the same conditions showed a significant and broad absorption peaks. In addition, a displacement of band absorption towards longer wavelengths has been observed, indicating an increase of AuNps sizes in concordance with the XRD results.

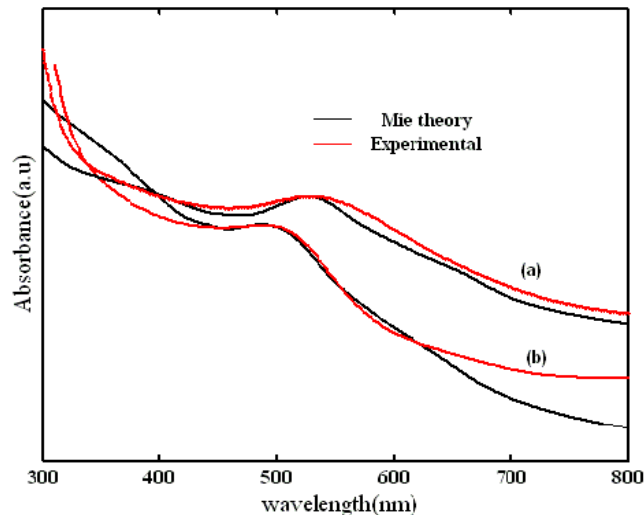


Fig. 6: Experimental and Mie simulated optical absorption spectra for Au/Al<sub>2</sub>O<sub>3</sub> films (a) Au target (2.6%), (b) Au target (1.3%).

The measured absorption spectra were simulated, based on the theoretical model described previously (combination of Eq. (1) and Eq. (2)). Fig.6 shows the experimental spectra of Au/Al<sub>2</sub>O<sub>3</sub> and their simulated curves. These fitting allowed us to evaluate, the gold particle size, the wavelength of the SPR band absorption spectra and the refractive index of the matrix. It was found that the plasmon peak position vary from 500 nm to 530nm, the size increases from 2.4 nm to 3.29 nm and the refractive index of the matrix varies from 1.76 to 1.84 when  $r_{\text{Au/Al}_2\text{O}_3}$  increases from 1.3% to 2.6%. In fact, probably both particle size and matrix refractive index affect the surface plasmon absorption

#### IV. CONCLUSION

In this work, Au/SiO<sub>2</sub> and Au/Al<sub>2</sub>O<sub>3</sub> nanocomposite films have been prepared by RF-sputtering technique, at the same deposition parameters. The structural and optical investigation of the composite films shows distinct results. Particularly, the size of Au particles in alumina matrix is larger than those of silica, whose remaining lower than 2nm. Degradation in the optical transmission spectra and shift to longer wavelength of absorption edge is more marked in the visible range in the case of alumina than silica matrix. Particularly, transparency located in the visible is more modified. Surface Plasmon resonance peak position characteristic of Au nanoparticles is only observed in Au/Al<sub>2</sub>O<sub>3</sub> films.

#### ACKNOWLEDGMENTS

We are grateful to Professor M.J.M. Gomes from the *Centre of Physics, University of Minho, Portugal*, for the experimental support.

#### REFERENCES

- [1] M.C. Daniel, D .Astruc, "Gold nanoparticles: assembly, supramolecular chemistry, quantum-size-related properties, and applications toward biology, catalysis, and nanotechnology," vol.104, pp.293-346, 2004.
- [2] S.J. Guo, E.K. Wang , "Synthesis and electrochemical applications of gold nanoparticles," *Analytica Chimica Acta*, vol. 598, pp. 181-192, 2007
- [3] E Boisselier, D Astruc , "Gold nanoparticles in nanomedicine: preparations, imaging, diagnostics, therapies and toxicity," *Chemical society reviews*, vol. 38, pp. 1759-1782,2009.
- [4] S.H. Radwan, H.M.E. Azzazy, "Gold nanoparticles for molecular diagnostics," *Expert review of molecular diagnostics*, vol.9, pp.511-524,2009.
- [5] W. R. Algar, M. Massey, U. J. Krull, "The application of quantum dots, gold nanoparticles and molecular switches to optical nucleic-acid diagnostics," *Trends in Analytical Chemistry*, vol. 28, pp. 292-306,2009.
- [6] W.E .Bawarski, E .Chidlowsky, D.J .Bharali, S.A .Mousa, "Emerging nanopharmaceuticals," *Nanomedicine: Nanotechnology, Biology and Medicine*, vol.4, pp. 273-282, 2008.
- [7] K.L. Kelly, E. Coronado, L.L. Zhao and G.C. Schatz, "The optical properties of metal nanoparticles: the influence of size, shape, and dielectric environment," *The Journal of Physical Chemistry. B*, vol. 107, pp. 668–677, 2003
- [8] C.F. Bohren and D.R. Huffman, *Absorption and Scattering of Light by Small Particles*, John Wiley & Sons, Inc., New York, 1983.
- [9] D. Dalacu, L. Martinu, "Spectroellipsometric characterization of plasma-deposited Au/SiO<sub>2</sub> nanocomposite films," *Journal of Applied Physics*, vol.87, pp.228-235, 2000.
- [10] C. Noguez, "Surface Plasmons on Metal Nanoparticles: The Influence of Shape and Physical Environment," *The Journal of Physical Chemistry C*, vol.111, pp .3806-3819, 2007.
- [11] S. Link, M.A. EL-Sayed, "Shape and size dependence of radiative, non-radiative and photothermal properties of gold nanocrystals," *International Reviews in Physical Chemistry*, vol.19, pp. 409-453, 2000.

- [12] G. Mie, "Beitrage zur Optik truber Medien, speziell kolloidaler Metallosungen," *Ann. Phys.*, vol. 25, pp. 377-445, 1908.
- [13] L.M. Liz-Marzan et al., *Handbook of Surfaces and Interfaces of Materials: Core-Shell Nanoparticles and Assemblies Thereof*, vol. 3, Chap. 5, Academic Press, San Diego, 2001.
- [14] S. Link and M.A. El-Sayed, "Spectral Properties and Relaxation Dynamics of Surface Plasmon Electronic Oscillations in Gold and Silver Nanodots and Nanorods," *J. Phys. Chem. B*, vol. 103, pp. 8410-8426, 1999
- [15] U. Kreibig and L. Genzel, "Optical absorption of small metallic particles," *Surf. Sci.*, vol. 156, pp. 678-700, 1985.
- [16] P. Mulvaney, "Surface Plasmon spectroscopy of nanosized metal particles," *Langmuir*, vol. 12, pp. 788-800, 1996.
- [17] H. Hovel, S. Fritz, A. Hilger, U. Kreibig, M. Vollmer, "Width of cluster plasmon resonances: bulk dielectric functions and chemical interface damping," *Phys. Rev. B*, vol.48, p.p.18178-18188, 1993.
- [18] J. Borges, F. Vaz, L. Marques, "AlN<sub>x</sub>O<sub>y</sub> thin films deposited by DC reactive magnetron sputtering," *Appl. Surf. Sci.*, vol. 257, pp. 1478-1483, 2010
- [19] J. Borges, N.P. Barradas, E. Alves, M.F. Beaufort, D. Eyidi, F. Vaz, L. Marques, "Influence of stoichiometry and structure on the optical properties of AlN<sub>x</sub>O<sub>y</sub> films," *J. Phys. D. Appl. Phys.*, vol. 46, p p. 015305-015315, 2013.
- [20] G. Eranna, B.C. Joshi, D.P. Runthala, R.P. Gupta, "Oxide materials for development of integrated gas sensors - a comprehensive review," *Crit. Rev. Solid State Mater. Sci.*, vol.29, pp.111-188, 2004.
- [21] K. Toki, K. Kusakabe, T. Odani, S. Kobuna, Y. Shimizu, "Deposition of SiO<sub>2</sub> and Ta<sub>2</sub>O<sub>5</sub> films by electron-beam-excited plasma ion plating," *Thin Solid Films*, vol.281-282,pp. 401-403, 1 August 1996.
- [22] T. Oyama, H. Ohsaki, Y. Tachibana, Y. Hayashi, Y. Ono, N. Horie, "A new layer system of anti-reflective coating for cathode ray tubes," *Thin Solid Films*, vol.351, pp. 235-240, 30 August 1999.
- [23] K. Takahiro, S. Oizumi, K. Morimoto, K. Kawatsura, T. Isshiki, K. Nishio, et al, "Application of X-ray photoelectrospectroscopy to characterization of Au nanoparticles formed by ion implantation into SiO<sub>2</sub>," *Appl. Sur. Sci.*, vol. 256, pp.1061-1064, 2009.
- [24] T. Cesca, C. Maurizio, B. Kalinic, C. Scian, E. Trave, G. Battaglin, P. Mazzoldi, G. Mattei, "Luminescent ultra-small gold nanoparticles obtained by ion implantation in silica," *Nucl. Instr. Meth. Phys. Res. Sec. B: Beam Inter. Mater. Atoms*, vol.326, pp.7-10, 2014.
- [25] D. Dhara, B. Sundaravel, T.R. Ravindran, K.G.M .Nair, C. David, B. K. Panigrahi, P. Magudapathy, K.H. Chen, "Spill out effect in gold nanoclusters embedded in c-Al<sub>2</sub>O<sub>3</sub> (0001) matrix," *Chem. Phys. Lett.*, vol. 399, pp.354-358, 2004.
- [26] M. Ohkubo, N. Susuki, "Morphology of small gold crystals formed inside sapphire by ion implantation," *Philos. Mag. Lett.*, vol. 57, pp. 261-265, 1988.
- [27] D. O .Henderson, R. Mu, Y .S. Tung, M. A. George, A. Burger, S.H. Morgan, C.W. White, R. A. Zuhr, R.H. Magruder, "Atomic force microscopy of Au implanted in sapphire," *J. Vac. Sci. Technol. B.*, vol. 13, pp. 1198-1202, 1995.
- [28] C. Margues, E. Alves, R.C. da Silver, M.R. Silva, A.L. Stepanov, "Optical changes induced by high fluence implantation of Au ions on sapphire," *Nucl. Instrum. Methods Phys. Res. B.*, vol.208, pp. 139-144, 2004.
- [29] M.C. Ferrara, L. Mirengi, A. Mevoli, L. Tapfer, "Synthesis and characterization of sol-gel silica films doped with size-selected gold nanoparticles," *Nanotech.*, vol. 19, pp. 65706-65714, 2008.
- [30] Y. Hosoya, T. Suga, T. Yanagawa, Y. Kurokawa, "Linear and nonlinear optical properties of sol-gel-derived Au nanometer-particle-doped alumina," *J. Appl. Phys.*, vol .81, pp. 1475-1480, 1997.
- [31] S. Muto, T. Kubo, Y. Kurokawa, K. Suzuki, "Third-order nonlinear optical properties of Disperse Red 1 and Au nanometer-size particle-doped alumina films prepared by the sol-gel method," *Thin Solid Films*, vol. 322, pp. 233-237, 1998.
- [32] J. Lermé, B. Palpant, B. Prével, E. Cottancin, M. Pellarin, M. Treilleux, J.L. Vialle, A. Perez, M. Broyer, "Optical properties of gold metal clusters: A time-dependent local-density- approximation investigation," *Eur. Phys. J.*, vol.4, pp. 95-108, 1998.
- [33] B. Palpant, B. Prével, J. Lermé, E. Cottancin, M. Pellarin, M. Treilleux, A. Perez, J.L. Vialle, M. Broyer, "Optical properties of gold clusters in the size range 2-4 nm," *Phys. Rev. B.*, vol. 57, pp.1963-1970,1998.
- [34] E. Cottancin, J. Lermé, M. Gaudry, M. Pellarin, J.L. Vialle, M. Broyer, B. Prével, M. Treilleux, P. Mélinon, "Size effects in the optical properties of Au<sub>n</sub>Ag<sub>n</sub> embedded clusters," *Phys. Rev. B.*, vol. 62, pp. 5179-5185, 2000.
- [35] M. Gaudry, J. Lermé, E. Cottancin, M. Pellarin, J. -L. Vialle, M. Broyer, B. Prével, M. Treilleux, P. Mélinon, "Optical properties of (AuxAg1-x)<sub>n</sub> clusters embedded in alumina: Evolution with size and stoichiometry," *Phys. Rev. B*, vol. 64: 085407/1-085407/7, 2001.
- [36] C.H. Kerboua, J.M. Lamarre, L. Martinu, S. Roorda, "Deformation, alignment and anisotropic optical properties of gold nanoparticles embedded in silica," *Nucl. Instr. Meth. Phys. Res. B*, vol, 257, pp.42-46, 2007.
- [37] J.M. Lamarre, Z. Yu, C. Harkati, S. Roorda, L. Martinu, "Optical and microstructural properties of nanocomposite Au/SiO<sub>2</sub> films containing particles deformed by heavy ion irradiation," *Thin Sol. Films*, vol.479, pp.232-237, 2005.
- [38] H.B. Liao, R.F. Xiao, J.S. Fu, P. Yu, G.K. Wong, P. Sheng, "Large third-order optical nonlinearity in Au: SiO<sub>2</sub> composite films near the percolation threshold," *Appl. Phys. Lett.*, vol.70, pp. 1-3, 1997.

- [39] I. Tanahashi, Y. Manabe, T. Tohda, S. Sasaki, A. Nakamura, "Optical nonlinearities of Au/SiO<sub>2</sub> composite thin films prepared by a sputtering method," *J. Appl. Phys.*, vol.79, pp. 1244-1249, 1996.
- [40] K.H Jung, J.W. Yoon, N. Koshizaki, Y.S. Kwon, "Fabrication and characterization of Au/SiO<sub>2</sub> nanocomposite films grown by radio-frequency cosputtering," *Curr. Appl. Phys.*, vol. 8, pp.761-765, 2008.
- [41] G.Q. Yu, B.K. Tay, Z.W. Zhao, X.W. Sun, Y.Q. Fu, Ion beam co-sputtering deposition of Au/SiO<sub>2</sub> nanocomposites, *Phys. E. Low-dim. Syst. Nanostr.*, vol. 27, pp.362-368, 2005.
- [42] B. Zhuo, Y. Li, S. Teng, A. Yang, "Films, fabrication and characterization of Au/SiO<sub>2</sub> nanocomposite films," *Appl. Sur. Sci.*, vol. 256, pp. 3305-3308, 2010.
- [43] P. Sangpour, O. Akhavan, A.Z. Moshfegh, M. Roozbehi, "Formation of gold nanoparticles in heat-treated reactive co-sputtered Au-SiO<sub>2</sub> thin films," *Appl. Surf. Sci.*, vol. 254, pp.286-290, 2007.
- [44] F. Ruffino, M.G. Grimaldi, C. Bongiorno, F. Giannazzo, F. Roccaforte, V. Raineri, "Microstructure of Au nanoclusters formed in and on SiO<sub>2</sub>," *Superl. Microstruct.*, vol.44, pp. 588-598, 2008.
- [45] H.B. Liao, W. Weijia, G.K.L. Wong, "Preparation and optical characterization of Au/SiO<sub>2</sub> composite films with multilayer structure," *J. Appl. Phys.*, vol.93, pp. 4485-4488, 2003.
- [46] S. Debrus, J. Lafait, M. May, N. Pinçon, D. Prot, C. Sella, J. Venturini, "Z-scan determination of the third-order optical nonlinearity of gold: silica nanocomposites," *J. Appl. Phys.*, vol. 88, pp.4469-4475, 2000.
- [47] N. Pinçon, B. Palpant, D. Prot, E. Charron, S. Debrus, "Third-order nonlinear optical response of Au:SiO<sub>2</sub> thin films: Influence of gold nanoparticle concentration and morphologic parameters," *Eur. Phys. J. D*, vol. 19, pp.395-402, 2002.
- [48] A. Belahmar, A. Chouiyakh, "Effect of post-annealing on structural and optical properties of gold nanoparticles embedded in silica films grown by RF- sputtering," *Adv. Phys. Theory. Appl.*, vol.15, pp. 38-46, 2003.
- [49] A. Belahmar, A. Chouiyakh, "Influence of the fabrication conditions on the formation and properties of gold nanoparticles in alumina matrix produced by cosputtering," *Int. J. Nano. Mater. Sci.*, vol. 3, pp. 16-29, 2014.
- [50] A. Belahmar, A. Chouiyakh, "Investigation of surface plasmon resonance and optical band gap energy in gold/silica composite films prepared by rf-sputtering," *Int. J. Nanosci. Tech.*, vol. 2, pp.81-84, 2016.
- [51] A. Belahmar, A. Chouiyakh, "Sputtering Synthesis and Thermal Annealing Effect on Gold Nanoparticles in Al<sub>2</sub>O<sub>3</sub> Matrix," *Journal of Nanoscience and Technology*, vol. 2, pp. 100-103, 2016.
- [52] H. B. Liao, R.F. Xiao, J. S. Fu, G. K. L. Wong, "Large third-order nonlinear optical susceptibility of Au-Al<sub>2</sub>O<sub>3</sub> composite films near the resonant frequency," *Appl. Phys. B*, vol. 65, pp. 673-676, 1997.
- [53] J. Wang, W.M. Lau, Q. Li, "Effects of particle size and spacing on the optical properties of gold nanocrystals in alumina," *J. Appl. Phys.*, vol. 97, pp. 114303(3) - 114303(8), 2005.
- [54] J. Garcia-Serrano, U. Pal, "Synthesis and characterization of Au nanoparticles in Al<sub>2</sub>O<sub>3</sub> matrix," *Int. J. Hydrogen Energy*, vol. 82, pp. 637-640, 2003.
- [55] J. Tauc, *Amorphous and liquid semiconductors*, Plenum, London, 1974.
- [56] E.D. Palik, *Handbook of Optical Constants of Solids III*, Academic Press, New York, 1991.
- [57] U. Kreibig, M. Vollmer, *Optical Properties of Metal Clusters*, Springer Series in Material Science, vol. 25. Springer, Berlin, 1995.
- [58] K.-J. Berg, A. Berger, H. Hofmeister, "Small silver particles in glass surface layers produced by sodium-silver ion exchange—their concentration and size depth profile," *Z. Phys. D*, vol. 20, pp.309-311, 1991.
- [59] A. Hilger, M. Tenfelde, U. Kreibig, "Silver nanoparticles deposited on dielectric surfaces," *Appl. Phys. B*, vol. 73, pp. 361-372, 2001.
- [60] B. Lamprecht, A. Leitner, F.G. Ausseneg, "Femtosecond decay-time measurement of electron-plasma oscillation in nanolithographically designed silver particles," *Appl. Phys. B*, vol. 64, pp. 269-272, 1997.
- [61] H. Hofmeister, W.G. Drost, A. Berger, "Oriented prolate silver particles in glass characteristics of novel dichroic polarizers," *Nanostruct. Mater.*, vol.12, pp. 207-210, 1999.
- [62] G. A. Rance, D. H. Marsh, A. N. Khlobystov, "Extinction coefficient analysis of small alkanethiolate-stabilised gold nanoparticles," *Chemical Physics Letters*, vol.460, pp. 230-236, 2008.